

# A Switched-capacitor Neural Preamplifier with an Adjustable Pass-band for Fast Recovery following Stimulation

R. Gusmeroli, *Student Member, IEEE*, A. Bonfanti, T. Borghi, *Student Member, IEEE*,  
 A. S. Spinelli, *Member, IEEE*, and G. Baranauskas, *Member, IEEE*

**Abstract**—For extracellular recordings from neurons, it is desirable to use the same electrode for stimulation as well as for recording. Since neural preamplifiers usually exhibit high-pass filtering at frequencies as low as 0.1 Hz, the recovery from saturation is typically very slow. Consequently, following stimulation, no signal can be detected for up to several seconds. This is an unacceptable slow response of the preamplifier because the majority of neurons fires action potentials within first milliseconds following stimulation. Here we propose to use a switched-capacitor preamplifier with adjustable pass-band for fast recovery from saturation caused by stimulation via the recording electrode. The idea was tested in a real preamplifier manufactured with a standard CMOS technology ( $0.35\text{ }\mu\text{m}$ ). In control conditions, the high-pass filter was set to 100 Hz and, during stimulation, was shifted to 10 kHz. Such a shift allows the reduction of the recovery time from tens of milliseconds to sub-millisecond range.

## I. INTRODUCTION

Extracellular recording of action potentials (AP) is a widely used technique to non-invasively monitor neurons in animals and during certain surgical procedures in humans [1]. While spontaneous activity or responses to natural stimuli can provide much information about neuronal coding, electrical stimulation permits to probe the connections of neurons and compares responses evoked by natural stimuli to local electrical stimulation. In addition, such stimulation may provide a two-way interaction for the brain-machine interfaces [2]. For all these applications, local stimulation provide the best conditions for analysis, making desirable to adopt the same electrode for stimulation as well as for recording [1], [3], [4]. This is an especially attractive solution when compact integrated devices are considered.

However, such a configuration poses a severe technical challenge. The amplitude of the AP recorded with an extracellular electrode is typically of the order of  $100\text{ }\mu\text{V}$  or less and must therefore be properly amplified [5]–[7]. Meanwhile, the amplitude of the electrical stimulus pulse is usually of the order of 1 V. If such large signal is fed into the input of the neuronal amplifier that has an amplification factor of 1000 – 5000, the amplifier is saturated even if the input is decoupled from the DC part of the signal.

The authors are with the Dipartimento di Elettronica e Informazione, Politecnico di Milano – IU.NET, piazza L. da Vinci, 32 20133 Milano, Italy.

G. Baranauskas is also with Dipartimento di Chimica, Materiali e Ingegneria Chimica “G. Natta”, Politecnico di Milano, Milano, Italy.

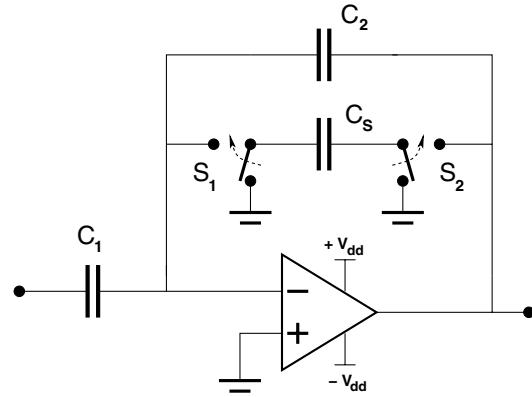


Fig. 1. Schematic diagram of the SC high-pass filter. Switches  $S_1$  and  $S_2$  are implemented with standard CMOS pass-transistors and commute at clock frequency  $f_{ck}$ .

The recovery from saturation is largely determined by the cut-off frequency  $f_L$  of the high-pass filter that decouples the amplifier from the input offset. Typical values of  $f_L$  are around 10 – 100 Hz [7]–[9], which corresponds to a recovery time of the order of 2 – 100 ms. Such a slow recovery prevents the collection of the response data from the stimulation electrode, as a large fraction of the neuronal response occurs within less than 10 ms following the stimulus [4], [10].

In this work, we show results of a low-power switched-capacitor preamplifier and stimulation circuit where the cut-off frequency of the high-pass filter can be dynamically adjusted to speed up the recovery from saturation. In particular, the cut-off frequency was increased during and soon after the stimulation phase, leading to a recovery time as low as  $450\text{ }\mu\text{s}$ . The integrated circuit was realized in CMOS  $0.35\text{ }\mu\text{m}$  technology and features a gain of 20 dB with an input rms noise of  $10\text{ }\mu\text{V}$  in the 100 Hz – 10 kHz bandwidth, and can thus be efficiently used as a preamplifier to record APs with extracellular electrodes in many applications.

## II. PREAMPLIFIER DESIGN

### A. Switched-capacitor high-pass filter

The integrated neural preamplifier is based on the so-called “switched-capacitor” (SC) technique [11]. This approach allows to implement a variety of tunable filters without using resistors, and has a number of advantages such as the *effective use of silicon area* (long time constants can be

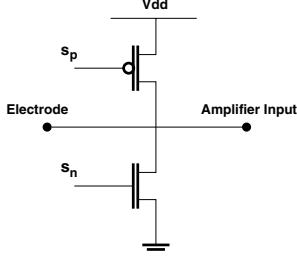


Fig. 2. Integrated circuit used for stimulation: the electrode can be either pulled up or down using the control signals  $s_p$  and  $s_n$ , respectively.

attained employing small areas of the chip) and the *flexibility*, due to the dependence of the filter parameters on the clock frequency. In this work, the latter feature was exploited to dynamically increase the high-pass pole frequency when fast recovery was needed. The scheme of the SC preamplifier is shown in Fig. 1. In terms of the equivalent continuous-time filter, the circuit works as a high-pass filter where the mid-band gain  $G$  and the high-pass pole frequency ( $f_L$ ) can be related to the circuit components as:

$$G = -\frac{C_1}{C_2} \quad f_L = \frac{f_{ck} C_s}{2\pi C_2},$$

where  $f_{ck}$  is the clock frequency at which the switches  $S_1$  and  $S_2$  are driven. The direct relationship between  $f_L$  and  $f_{ck}$  allows to shift the high-pass pole by a simple clock frequency variation. Parameter values employed here are  $C_1 = 40 \text{ pF}$ ,  $C_2 = 4 \text{ pF}$ , and  $C_s = 50 \text{ fF}$ .

### B. Stimulation circuit

We have designed a simple circuit for stimulating the cells via the same electrode that is employed for readout, which is shown in Fig. 2. In this circuitry, two MOS switches are connected to power supplies and controlled by the signals  $s_p$  and  $s_n$ . All possible operating modes of the circuit are summarized in the following table:

$s_p$	$s_n$	Mode
0	0	Stimulation @ $V_{dd}$
0	1	-
1	0	Readout (no stimulation)
1	1	Stimulation @ 0 V

### C. Test chip

To experimentally test the circuit performance, a test chip was manufactured with a standard  $0.35 \mu\text{m}$  CMOS technology (Austriamicrosystems C35B4C3, with supply voltages of  $\pm 1.65 \text{ V}$ ), and is shown in Fig. 3. The preamplifier (light region) was realized within a larger chip having dimensions of  $2 \text{ mm} \times 2.5 \text{ mm}$ , with input/stimulus electrode on the left and output and supply electrodes on the right: such a choice eases the electrical isolation of output and power supply pads from the culture medium. The switches  $S_1$  and

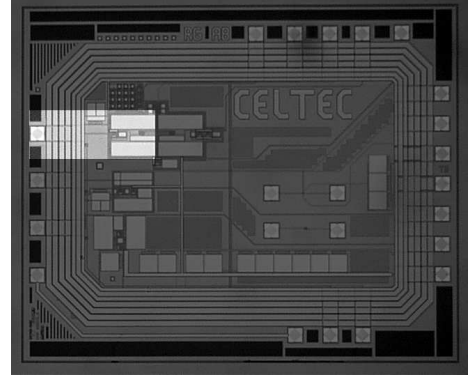


Fig. 3. Microphotograph of the integrated test-chip. The highlighted region represents the neural preamplifier and the readout electrode (other preamplifier schemes were integrated for testing). Overall chip size is  $2 \times 2.5 \text{ mm}^2$

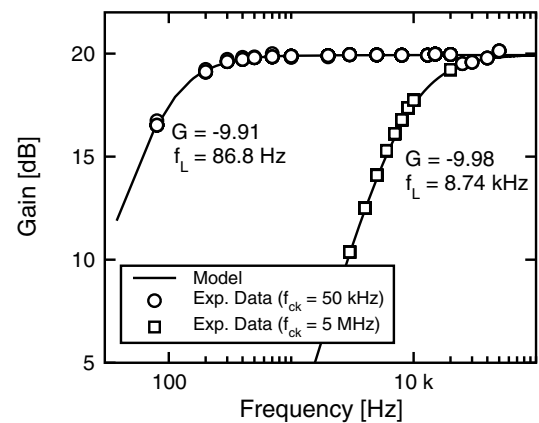


Fig. 4. Frequency response of the preamplifier for  $f_{ck} = 50 \text{ kHz}$  (circles) and  $f_{ck} = 5 \text{ MHz}$  (squares). Continuous line represents a fit of a continuous time high-pass filter model (parameters  $G$  and  $f_L$  are given in the figure)

$S_2$  were implemented with standard CMOS pass-transistors. The resulting preamplifier characteristics are:

$$G = -10 \quad f_L = 2 \times 10^{-3} \cdot f_{ck}.$$

Note that an amplification factor as low as 10 was deliberately chosen, in order to directly observe the recovery process while minimizing the effects of the input noise. However, the actual amplification factor will not affect any of our conclusions.  $f_L$  was set to a value around 100 Hz, close to the typical values found in neural preamplifiers. In our scheme, such a value can be achieved with a clock frequency  $f_{ck} = 50 \text{ kHz}$ .

## III. EXPERIMENTAL RESULTS

### A. Transfer function

The measured amplitude of the transfer function for  $f_{ck} = 50 \text{ kHz}$  and  $f_{ck} = 5 \text{ MHz}$  are presented in Fig. 4. In the same figure, a fit function corresponding to the following continuous-time formula is shown:

$$H(s) = G \frac{s}{s + 2\pi f_L}.$$

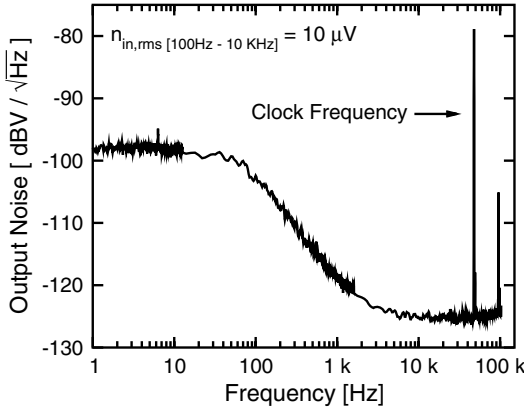


Fig. 5. Output noise spectrum of the preamplifier. The clock frequency is  $f_{ck} = 50$  kHz.

The table below shows that the fit parameters are in good agreement with the predicted ones:

$f_{ck}$	$G$	$f_L$	$f_L/f_{ck}$
50 kHz	-9.91	86.6 Hz	$1.7 \times 10^{-3}$
5 MHz	-9.98	8.74 kHz	$1.7 \times 10^{-3}$

### B. Noise

To assess the circuit sensitivity, the output noise spectrum was measured and is shown in Fig. 5. Note a strong peak around 50 kHz corresponding to the clock frequency, which is nevertheless outside the frequency band of a typical application and can be reduced by employing a notch filter. The rms value of the noise referred to the input in the frequency band (100 Hz – 10 kHz) is 10  $\mu$ V, which decreases to 7  $\mu$ V if a narrower band (500 Hz – 10 kHz) is considered.

### C. Recovery following stimulation

One of the advantages of the designed preamplifier is the possibility to achieve an extremely fast recovery after stimulation. The idea is to use a time window, centered around the stimulation period, where the clock frequency is raised, shifting  $f_L$  to high frequencies and increasing the recovery speed. Such an interval is hereafter referred to as the *fast-mode window*.

To verify this idea, the circuit described in Sec. II-B was used for stimulation. Only positive-voltage stimulations were applied, meaning that only the signal  $s_p$  was changed during the test, while keeping  $s_n$  at 0. The duration of stimulation was set to 200  $\mu$ s. A signal was then applied at the input via a pulse generator, 1 ms after the end of stimulation. The shape of this signal was chosen to approximately represent the shape of a typical extra-cellular AP, although its amplitude, 100 mV, was chosen much larger because of the limited amplification factor (10 $\times$ ) that was used here. Again, the actual value of the amplification factor will not affect any of our conclusions, as what we want to demonstrate here is

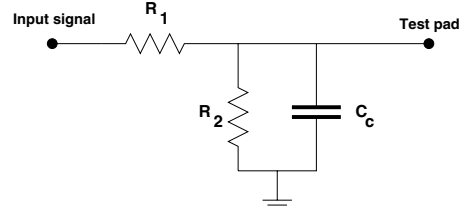


Fig. 6. Circuit used to simulate a typical impedance of the electrode/solution interface. Circuit parameters are:  $R_1 = R_2 = 100$  k $\Omega$  and  $C_c = 1$  nF.

the recovery capability of the circuit, which is independent of the amplifier gain.

To reproduce as accurately as possible the real conditions of operation, we inserted an impedance in series to the electrode input, to simulate the electrical behavior of the electrode-solution interface. This impedance is shown in Fig. 6, with values in agreement with [12].

Fig. 7 and 8 show the recovery performance of the circuit when the clock frequency is held constant (*i.e.*, the amplifier is used in its standard way, similarly to a traditional amplifier), and when it is dynamically changed during operation, respectively. Note that, in the standard mode of operation, the amplified signal is superimposed onto a slow recovery, complicating its accurate measurement. In fact, whenever the preamplifier is followed by a second stage with a sufficient gain, the final output will remain saturated and no signal will be revealed until the preamplifier output will drop to a value low enough. According to Fig. 7, for an additional amplification factor of 100 $\times$ , such a saturated state may last several ms, depending on the time constant of the input filter.

A much better performance is achieved if  $f_{ck}$  is increased during stimulation. In our case,  $f_{ck}$  was raised to 5 MHz 100  $\mu$ s before the beginning of stimulation and brought back to 50 kHz 600  $\mu$ s after its end. It can be seen that the preamplifier is indeed able to recover completely after less than 1 ms following the stimulation, allowing to correctly detect the input signal. Such a result is a consequence of the fast time constant of the filter in the first hundreds of  $\mu$ s after the stimulation signal.

### D. Fast-mode window optimization

To evaluate the optimal duration of the fast window, we measured the residual output voltage for different fast-mode window durations. Test signals were the same as in Sec. III-C but without any simulated AP. Fig. 9 shows the residual voltage at the amplifier output 100  $\mu$ s after the clock reset (open circles), plotted against the time after the stimulation phase. For comparison, the output voltage was also measured without the fast window adjustment under the same stimulus conditions (solid circles). For a maximum output voltage of 10 mV, our design permits signal readout less than 450  $\mu$ s after stimulation, which is a value low enough for typical applications.

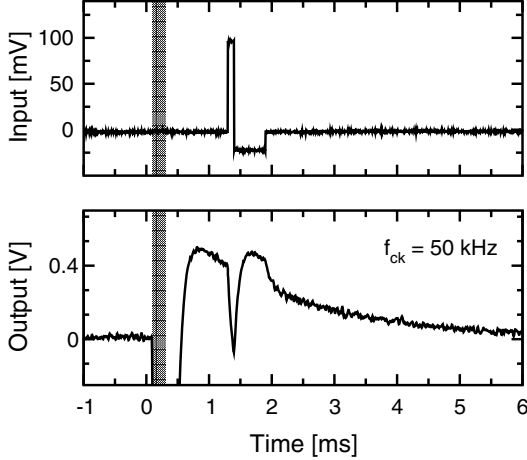


Fig. 7. Input and output signals of the preamplifier during and following stimulation, for constant  $f_{ck}$ . The shaded area represents the stimulation time. Note slow recovery from saturation superimposed onto the amplifier signal.

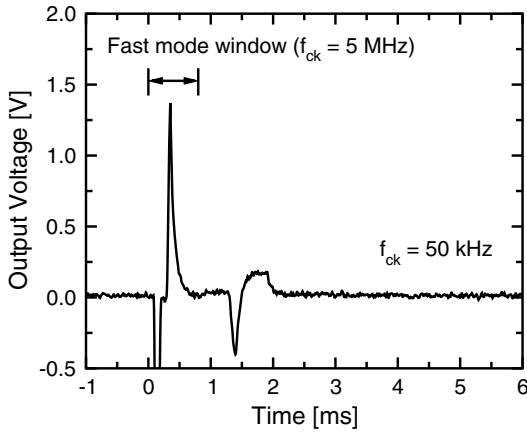


Fig. 8. Output signal of the preamplifier when  $f_{ck}$  is dynamically changed. Note fast recovery from saturation.

#### IV. CONCLUSIONS

We have designed a switched-capacitor preamplifier employing a dynamically adjustable high-pass filter time constant. The time needed to recover the amplifier output from saturation after stimulation is improved by a factor of about 10 with respect to conventional schemes. Other solutions for bandwidth adjustment can be used [7], but the adoption of a switched-capacitor amplifier allows very fast and large changes in the bandwidth that can be easily predicted according to the parameters of the scheme. This solution can eliminate the limitations posed by the preamplifier without compromising the requirements for low noise levels that are necessary to be achieved by neuronal amplifiers.

#### V. ACKNOWLEDGMENTS

The authors would like to acknowledge A. Lacaita, A. Cigada and R. Pietrabissa for helpful discussions and for

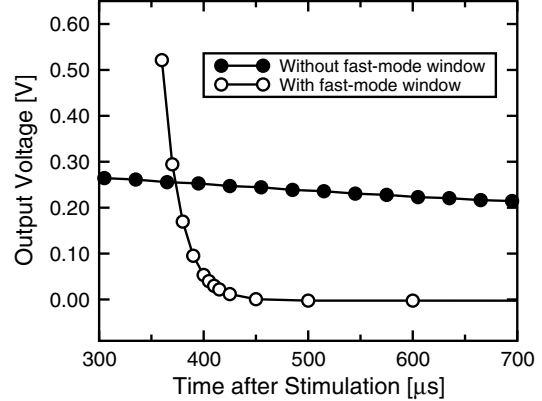


Fig. 9. Residual output voltage for different high- $f_{ck}$  time windows (open symbols). The output voltage at constant  $f_{ck}$  measured at the same time point after the end of stimulation, is also shown (filled symbols).

supporting this work, and V. Pecunia for his help in the test-chip characterization.

This work was partially supported by the Fondazione Cariplo, the “CelTec - Cells for Technology” project of the Politecnico di Milano, and by IIT (Italian Institute of Technology).

#### REFERENCES

- [1] E. N. Brown, R. E. Kass, and P. P. Mitra, “Multiple neural spike train data analysis: state-of-the-art and future challenges,” *Nature Neurosci.*, vol. 7, pp. 456–461, 2004.
- [2] M. A. Nicolelis, “Brain-machine interfaces to restore motor function and probe neural circuits,” *Nat. Rev. Neurosci.*, vol. 4, pp. 417–422, 2003.
- [3] G. Buzsaki, “Large-scale recording of neuronal ensembles,” *Nature Neurosci.*, vol. 7, pp. 446–451, 2004.
- [4] D. A. Wagenaar and S. M. Potter, “Real-time multichannel stimulus artifact suppression by local curve fitting,” *J. Neurosci. Methods*, vol. 120, pp. 113–120, 2002.
- [5] I. Obeid, J. C. Morizio, K. A. Moxon, M. A. Nicolelis, and P. D. Wolf, “Two multichannel integrated circuits for neural recording and signal processing,” *IEEE Trans. Biomed. Eng.*, no. 50, pp. 255–258, 2003.
- [6] R. H. Olsson, D. L. Buhl, A. M. Sirota, G. Buzsaki, and K. D. Wise, “Band-tunable and multiplexed integrated circuits for simultaneous recording and stimulation with microelectrode arrays,” *IEEE Trans. Biomed. Eng.*, vol. 52, pp. 1303–1311, 2005.
- [7] T. Horiuchi, T. Swindell, D. Sander, and P. Abshier, “A low-power CMOS neural amplifier with amplitude measurements for spike sorting,” in *Proc. ISCAS*, p. 2932, 2004.
- [8] F. Heer, W. Franks, A. Blau, S. Taschini, C. Ziegler, A. Hierlemann, and H. Baltes, “CMOS microelectrode array for the monitoring of electrogenic cells,” *Biosens. Bioelectron.*, vol. 20, no. 358–366, 2004.
- [9] W. R. Patterson, Y. K. Song, C. W. Bull, I. Ozden, A. P. Deangelis, C. Lay, J. L. McKay, A. V. Nurmikko, J. D. Donoghue, and B. W. Connors, “A microelectrode/microelectronic hybrid device for brain implantable neuroprosthetic applications,” *IEEE Trans. Biomed. Eng.*, vol. 51, pp. 1845–1853, 2004.
- [10] G. Raffaelli, C. Saviane, M. H. Mohajerani, P. Pedarzani, and E. Cherubini, “K potassium channels control transmitter release at CA3-CA3 synapses in the rat hippocampus,” *J. Physiol.*, vol. 557, pp. 147–57, 2004.
- [11] R. Gregorian and G. C. Temes, *Analog MOS Integrated Circuits for Signal Processing*. Wiley-Interscience, Apr 1986.
- [12] M. O. Heuschkel, M. Fejtl, M. Raggenbass, D. Bertrand, and P. Renaud, “A three-dimensional multi-electrode array for multi-site stimulation and recording in acute brain slices,” *J. Neurosci. Methods*, vol. 114, no. 135–148, 2002.